Published in: Journal of the European Ceramic Society (2009), vol. 29, iss. 11, pp. 2169-2175
Status: Postprint (Author's version)

Mullite coatings on ceramic substrates: Stabilisation of Al_2O_3-SiO_2 suspensions for spray drying of composite granules suitable for reactive plasma spraying

A. Schrijnemakers[a], S. André[b], G. Lumay[c], N. Vandewalle[c], F. Boschini[a,c], R. Cloots[a], B. Vertruyen[a]
[a] *LCIS/CMI, Chemistry Institute B6, University of Liège, B-4000 Liège, Belgium*
[b] *BCRC, Belgian Ceramic Research Center, B-7000 Mons, Belgium*
[c] *GRASP/APTIS, Physic Institute B5, University of Liège, B-4000 Liège, Belgium*

Abstract

The present work deals with the preparation of stable alumina + silica suspensions with high solid loading for the production of spray-dried composite powders. These composite powders are to be used for reactive plasma spraying whereby the formation of mullite and the coating on a ceramic substrate are achieved in a single step process. Electrostatic stabilisation of alumina and silica suspensions has been studied as a function of pH. Silica suspensions are most stable at basic pH whereas alumina suspensions are stable at acidic pH. The addition of ammonium polymethacrylate (APMA) makes it possible to stabilise alumina and prepare a stable 50 wt% alumina + silica suspension at pH 10. The optimum amounts of dispersant and binder have been determined by zeta potential, viscosity and sedimentation measurements. Spray drying of the suspension yields composite powders whose morphology, size distribution and flowability have been characterized before realizing reactive plasma spraying tests.

Keywords: D. Mullite; E. Refractories; A. Suspensions

1. Introduction

Plasma spraying is a well-known industrial technique, suitable to make metallic or ceramic coatings.[1] Oxide ceramic coatings are used to improve the resistance to corrosion, heat and wear of metal components.[2-6] For example, mullite ($3Al_2O_3 \bullet 2SiO_2$) ceramic coatings are being developed as thermal control coatings and as hard and abrasion-resistant thermal barrier coatings (TBC) for application in space.[7] During the plasma spraying process,[1] solid particles are injected into a plasma jet created either by a D.C. arc or by a R.F. field. The feedstock material is melted in the high temperature region of the plasma and the molten particles are accelerated until impact on the substrate. Then, rapid solidification of impacted droplets and deposit build up occur. The coating quality depends on various process parameters but also on the characteristics of the powder. Two kinds of ceramic powders are generally used for plasma spraying: "fused and crushed" or "agglomerated and sintered". The fused and crushed route[8] usually yields angular particles, whose poor flowability is a drawback in the case of plasma spraying. On the contrary, agglomerated powders with spherical morphologies and free flowability can be obtained by spray drying, a versatile industrial process during which a water-based suspension is transformed into a dry agglomerated powder by atomisation of the fluid feed material into a stream of hot air. Both the slurry properties (initial solid content, viscosity, etc.) and the drying conditions (atomiser design, drying temperature, etc.) are known to affect the morphology of the granules.[9-15] In the conventional plasma spraying technique of multicationic oxides, the granules of agglomerated powders are sintered prior to their use in the plasma spraying equipment. However, since optimized spray drying results in a homogeneous distribution of constituent materials, the composite granules can be used as-obtained for *reactive* plasma spraying. In this technique, the formation of the final compound by reaction of the individual oxides and the coating on a ceramic substrate are achieved in a single process.

The present study focuses on mullite ($Al_6Si_2O_{13}$), a traditional ceramic well-known for its excellent thermo-mechanical properties.[16] Literature papers relevant to the reactive plasma spraying of mullite from agglomerated precursors are scarce and concern the formation of amorphous particles[17] or flakes.[18] Our objective is to achieve the formation of crystallized mullite coatings by reactive plasma spraying of spray-dried Al_2O_3-SiO_2 composite granules. We report first on the preparation of the composite granules by spray drying of an alumina + silica suspension whose pH, dispersant content and binder content are optimized thanks to zeta potential,

sedimentation and viscosity measurements. Then the morphology, size distribution and flowability of the spray-dried powder are discussed. The final section presents the results of reactive plasma spraying tests.

2. Experimental

α-Al_2O_3 (average grain size 1.35 µm) and α-SiO_2 (average grain size 1.5 µm) were purchased from Alcan, France (ref P152SB) and Silicil Sifraco, France (ref C800), respectively. The anionic dispersant used for alumina stabilisation was an ammonium salt of polymethacrylic acid (APMA), available commercially with the trade name Darvan C and supplied by R.T. Vanderbilt Co. Norwalk, CT, USA as a 25 wt% aqueous solution with a molecular weight around 14,000 g/mol. Polyvinylic alcohol (PVA) and polyethylene glycol (PEG), respectively with a mean molecular weight of 61,000 and 400 g/mol were used as binders. Concentrations are given as weight% (wt%), referred to the solids loading, of the as-received product. Analytical reagent grade solutions of sodium hydroxide (1 mol/1) and hydrochloric acid (1 mol/1) were used to adjust the pH of the suspensions. The dilution of the suspensions by these additions was negligible. All solutions and suspensions were prepared with deionised water. Spray drying of the suspensions was performed in a Niro Mobile Minor spray dryer with a fountain-mode pneumatic atomisation system. During spray drying, air inlet temperature and compressed air flow were maintained to 190 °C and 40ml/min, respectively. Reactive plasma spraying experiments were carried out with a subsonic torch (nozzle diameter 8 mm), used in maximal power conditions (30 kW). The ceramic substrates were porous mullite pieces and the torch-substrate distance was 80 mm.

Zeta potential measurements were carried out on concentrated suspensions using an Acoustosizer II (Colloidal Dynamics). Freshly prepared suspensions were introduced in the cell to allow dynamic measurement with 20rpm circulation speed. The amplitude and phase shift of the acoustic signal are recorded in a dynamic mobility spectrum, from which zeta potential and particle size can be calculated.[19,20] Sedimentation measurements were performed using a Turbiscan MA 2000 (For-mulaction). 50 wt% suspensions were introduced in a vertical borosilicate glass tube. An optical head using near infrared light (850 nm) records the transmitted and back-scattered intensities as a function of height. The back scattering signal is maximum and the transmission is minimum for an opaque medium, and inversely for a limpid medium. Scans were recorded every 12min during 24 h. The first scan starts immediately after the transfer of the suspension into the tube. From these spectra it is possible to determine information such as the clarification rate.[21,22] The suspension viscosity was measured in a double concentric cell with a CS 10 Bohlin rheometer. Shear-stress measurements were carried out for shear rate ranging from 0.02 to 100s^{-1}.

A Siemens D5000 powder diffractometer (Cu K_α) and a Bruker D8 parallel beam diffractometer (Cu K_α) were used to characterize the crystallographic structure of the spray-dried powder and the plasma-sprayed coatings, respectively. Quantitative phase analysis of the calcined spray-dried powders was performed with the TOPAS Rietveld software package (Bruker). Microscopic characterization was carried out in a Philips XL30 FEG-ESEM scanning electron microscope. The particle size distribution (Malvern Mastersizer 2000) was measured on powder dispersed in water by sonication. Pycnometer Accupic 1330 (Micromeritics) was used to determine the apparent density of the powders through helium displacement. The powder fiowability was determined by a stress tap method as previously reported in ref. 23. The powder cohesion was characterized with an experimental set-up consisting in a short drum rotating around its (horizontal) central axis. The drum is half-filled with powder. The drum rotational speed is precisely controlled between 6 and 35 rpm. For each angular velocity, images are recorded with a CCD camera every 0.5 s during 25 s. A dedicated image processing algorithm tracks the position of the air/powder interface. The average interface position and the fluctuations around this average position are computed. The fluctuations (standard deviation) are related to the cohesion inside the powder. From the average interface position, the dynamic angle is measured in the centre of the flow.

3. Results and discussion

3.1. Suspension stabilisation

3.1.1. Zeta (ζ)-potential

In addition to sedimentation studies, the determination of the double layer characteristics by zeta (ζ)-potential measurements yields useful information concerning the stability of suspensions. In the present work, zeta

potential was measured by the Electrokinetic Sonic Amplitude (ESA) method. The advantage of this technique is that it does not require dilution of high solid content suspensions, at the opposite of other (esp., optical) methods, such as dynamic light scattering.[20]

Fig. 1 shows the influence of pH on the ζ-potential curves of 10wt% aqueous suspensions of SiO_2 and Al_2O_3 particles. The natural pH of the silica suspension is 8.3. The particles have a negative charge in the whole pH range from 2 to 12 and the most negative ζ-potential value (-80 mV) is obtained at pH 12 in agreement with ref. 23. The negative ζ-potential of silica particles can be explained by the formation of $\equiv SiO^-$ species.[25] In acidic media the negative surface charge decreases due to the progressive neutralization of $\equiv SiO^-$ groups and the isoelectric point (IEP) is reached near pH ~1.

The natural pH of the alumina suspension occurs at 9.2. At this pH, particles have a small negative ζ-potential (-11.7 mV), as also reported by Boufi et al.[24] The IEP of alumina is found to be at pH 8.3, in agreement with ref. 24-26 Below the IEP, the hydroxyl groups of alumina are protonated and the surface charge is dominated by $=Al\text{-}OH_2^+$ species. The maximum ζ-potential (+95.3 mV) is obtained at pH ~2. Above the IEP, the negative charge of the surface results from the formation of $=Al\text{-}O^-$ groups, which are generated by dissociation of the hydroxyl groups of alumina.

In view of the above, it is clear that the best electrostastic stabilisation occurs at basic pH for silica and at acidic pH for alumina. However mixing these suspensions would lead to floc-culation. In order to prepare suspensions containing both SiO_2 and Al_2O_3, silica and alumina particles must have the same sign of surface charge. This is the case at basic pH. At pH 10 (maximal value for preventing corrosion of the spray drying equipment), the SiO_2 suspension is stable but the ζ-potential of alumina is not sufficient to stabilise electrostatically the suspension. Therefore the stabilisation of the alumina suspension at pH 10 must be improved by means of a dispersant.

APMA is an anionic polyelectrolyte at all pH values in the range of pH 4-10.[27] At pH 10, APMA adsorption onto the alumina particle surface enhances the negative surface charge: the magnitude of the ζ-potential increases with APMA addition until it reaches the value of -70 mV for 0.3 wt% APMA. Further addition of APMA does not influence significantly the ζ-potential, indicating that maximum adsorption of APMA is reached at 0.3 wt% and that APMA excess remains unadsorbed in solution.[28] The value of 0.3 wt% of APMA is thus taken to be the optimum amount of dispersant required to stabilise the powder in these conditions.

Fig. 1. *pH dependence of the zeta-potential of silica and alumina suspensions.*

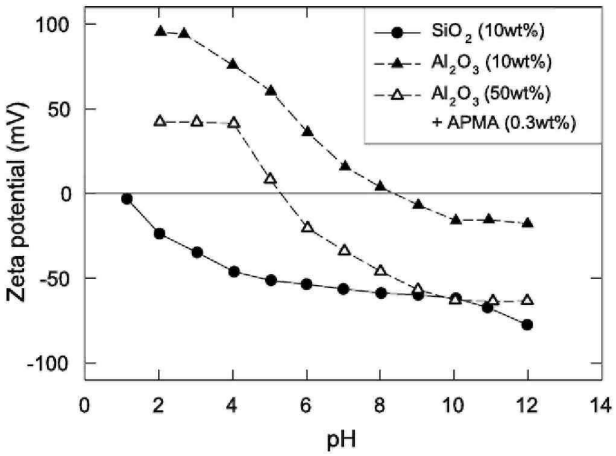

Fig. 1 shows the influence of pH on the ζ-potential of a 50 wt% alumina suspension containing 0.3 wt% APMA. Due to APMA adsorption on alumina particles, the IEP of Al_2O_3 is shifted from 8.3 to 5.3, as also observed by Beattie and co-workers.[28,29] At the IEP, the negative contribution from the polyelectrolyte car-boxylate compensates the positive contribution from $=AlOH_2^+$ groups. Below the IEP, carboxylate groups from APMA and free hydroxyl groups of alumina are protonated (-COOH and $=AlOH_2^+$), leading to a positive surface charge. Above the IEP, the anionic polyelectrolyte is ionised ($-COO^-$) and its adsorption on alumina results in negative ζ-potential values. The maximum negative ζ-potential value (-63 mV) is obtained for alkaline pH (from 10 to 12) where the APMA chains are fully ionised and repel each other.

The results of the zeta potential measurements are corroborated by particle size distribution data calculated from

the dynamic mobility spectrum obtained by the electroacoustic technique. Fig. 2 shows the particle size distribution in silica suspension (10 wt%), alumina suspension (10 wt%) and alumina suspension (50 wt%) with 0.3 wt% APMA. At pH 10, the apparent size of silica particles agrees well with the particle size of ~1.5µm estimated by scanning electron microscopy and laser diffraction measurements. At alkaline pH, the apparent size distribution of alumina particles is broad, reflecting agglomeration due to insufficient electrostatic repulsion. At pH 10, the addition of 0.3 wt% APMA to an agglomerated 50 wt% alumina suspension results in electrostatic dispersion and the particle size distribution curve narrows markedly.

Fig. 2. *Grain size distribution of silica and alumina suspensions (pH 10).*

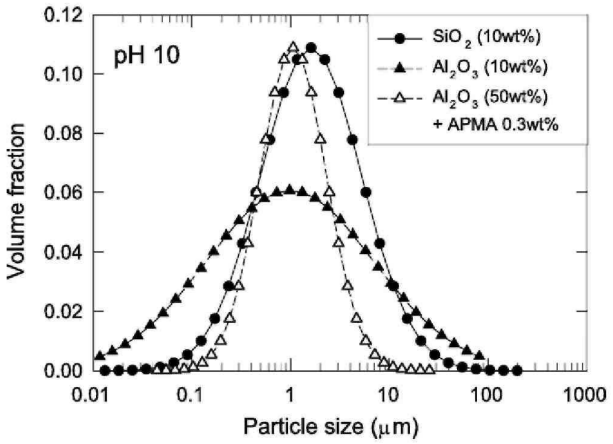

3.1.2. Sedimentation experiments

The stability of suspensions is frequently studied by sedimentation experiments using, for instance, turbidimetry. Sedimentation of concentrated suspensions cannot be monitored with the back-scattered signal because there is no peak corresponding to the sediment height.[20] Instead, the transmission signal is used in order to follow the evolution of clarification signal depth as a function of time. In the following experiments, the clarification signal depth was defined as the height of the liquid where transmission exceeds 2%.

Fig. 3 shows the clarification signal depth of a 50 wt% silica suspension as function of time for pH 10. In agreement with ζ-potential measurements, the suspension at pH 10 is rather stable and clarification is not observed before ~4.5 h. Data for a 50 wt% alumina suspension at pH 10 with 0.3 wt% APMA are shown in the same graph. As suggested by the zeta-potential and particle size distribution results, APMA addition stabilises alumina suspensions at basic pH: a delay of ~2.5 h before sedimentation is obtained for the optimum amount of APMA (0.3 wt%).

Fig. 3 also shows the sedimentation behaviour of a suspension containing both alumina and silica, prepared by mixing a alumina suspension at pH 10 containing 0.3 wt% APMA and a silica suspension at pH 10 in 3:2 Al:Si stoichiometric ratio. Since the surface charge of silica is negative, repulsion takes place between silica particles and the functional groups of anionic polyelectrolytes adsorbed on the surface of alumina particles.[24] Besides, no competition occurs between alumina and silica for APMA adsorption when they are mixed. The sedimentation starts after ~2.5h, as governed by the less stable component of the mixture, *i.e.,* alumina. This delay is sufficient for spray drying applications.

In view of the spray drying process, it is necessary to add a binder to the suspension in order to enhance the strength of the as-sprayed granules. Two binders have been considered in this work: polyethylene glycol and polyvinyl alcohol. At basic pH, these non-ionic binders are not expected to compete significantly with APMA for adsorption on the alumina particles.[30,31] However, Fig. 3 shows that addition of 2 wt% of binder to the alumina + silica suspension tends to improve slightly the stability, with the delay before settling reaching ~4h. Viscosity measurements (not shown) indicate that the short PEG chains have little effect on the suspension viscosity. On the contrary, the viscosity increases from ~5 mPas to ~12 mPas with addition of 2 wt% PVA, due to the introduction of high molecular weight macromolecules in the medium.[32] From these results, 2 wt% of binder is taken as a suitable amount for achieving appropriate suspension characteristics for spray drying, *i.e.,* low viscosity and sufficient stability.

Fig. 3. *Sedimentation of various 50 wt% suspensions (pH 10).*

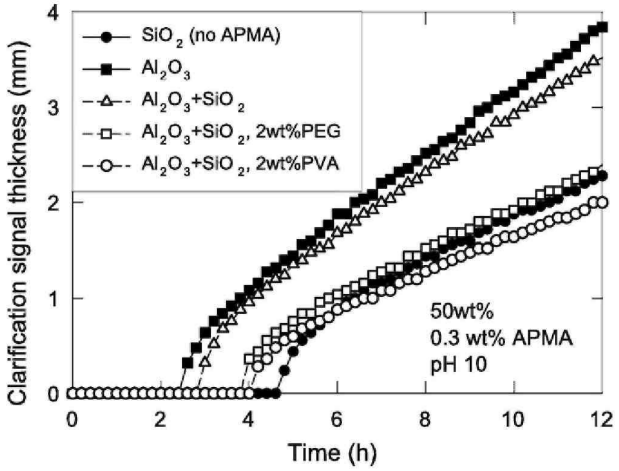

3.2. Spray drying and powder characterization

As discussed above, the Al_2O_3 + SiO_2 suspensions optimized for spray drying were prepared at pH 10 with Al_2O_3/SiO_2 molar ratio equal to 3/2 and with 0.3 wt% APMA. Suspensions were prepared with 65 wt% dry solid loading and two different binders (PEG or PVA, both 2 wt%). These suspensions (named PEG65 and PVA65 hereafter) were successfully spray-dried with the equipment and conditions described in Section 2. The Al_2O_3/SiO_2 ratio in the spray-dried granules was determined by Rietveld analysis of the XRD patterns and was found to agree with the ratio in the suspension. This confirms the stability of the suspension during the whole duration of the spray-drying process.

Fig. 4a shows the spherical morphology of the spray-dried composite powders. A micrograph of a cross-section through the spray-dried particles (Fig. 4b) shows that the granules are relatively dense and contain no internal voids. The powder size distribution data are given in Table 1. The mean size ($d_{0.5}$) of the as-sprayed granules increases from 80 to 100 µm when PVA is used instead of PEG as a binder, because suspensions containing PVA have higher viscosity and induce the formation of larger droplets during the atomisation.

The composite granules are to be used as feedstock material for plasma spraying, therefore it is desirable that these granules display good flowability, low inter-granule cohesion and high intra-granule cohesion. In order to make it easier to compare the properties, both composite powders were sieved to remove the largest particles (d> 160 µm) and obtain similar size distributions (see Table 1). The flowability of the composite powders has been characterized by a packing method.[23] The $n_{1/2}$ coefficient is defined as the number of taps needed to reach half of the density obtained after 500 taps. A low $n_{1/2}$ means that packing is fast, *i.e.*, the flowability is good. Table 1 gives the $n_{1/2}$ coefficient of the composite powders before and after sieving. In all cases the flowability seems rather good, with $n_{1/2}$ values below 10, probably due to the spherical morphology of the granules. Both before and after sieving, the composite granules prepared with PVA have the best flowability. The removal of the fraction of largest particles by sieving appears to decrease the flowability. Another parameter obtained from the packing experiment is the d_{500}/d_0 ratio, *i.e.*, the ratio between the density reached after application of 500 taps (d_{500}) and the density of the powder before the experiment starts (d_0). Interpretation of the d_{500}/d_0 data is not straightforward, because it depends on how far the initial arrangement of the powder (related to d_0) is from the optimal packing organisation (related to d_{500}). However, in the case of the sieved powders (see Table 1), the size distributions and the d_0 values (estimated independently by helium pycnometry) are similar. Therefore the somewhat higher d_{500}/d_0 ratio reported in Table 1 for the PEG65 sample suggests that the composite granules prepared with PEG do not behave as rigid spheres, but possibly deform or break. In order to investigate this point, the sieved samples have been characterized in the powder-drum setup (see Section 2 for details). Fig. 5 shows the dynamic angle and the standard deviation from the average interface position as functions of the rotational speed. At low rotational speed, the fact that the dynamic angle is smaller for PVA65 (~30°) than for PEG65 (~35°) confirms the better flowability of the granules prepared with PVA, as already observed in the packing experiment. Above ~20 rpm, the dynamic angle for the PEG65 sample increases markedly whereas the dynamic angle for the PVA65 sample does not depend very much on the rotational speed. This difference of behaviour is also found in the standard deviation data, which indicate that there are much more fluctuations around the average interface position in the case of the PEG65 sample. A measurement of the size distribution

after the powder-drum experiment clarifies the origin of these observations. The distribution curve of the PVA65 sample is not affected at all, as can be seen from the data in Table 1. On the contrary, the distribution curve for the PEG65 sample (Fig. 6) reveals the deterioration of the granules, with two secondary maxima centred on 0.6 and 11 µm. Obviously the stresses encountered by the granules in the packing and powder-drum experiments are not the same as those experienced in the powder feeder of the plasma spraying equipment. However the results clearly indicate that the intra-granule cohesion of the composite granules prepared with PEG is not as good as that of the granules prepared with PVA, possibly due to the smaller size of the PEG chains compared to PVA but also to their different glass transition temperatures (T_g). Indeed the mechanical properties of polymers are strongly dependent on their T_g.[33,34]

Fig. 4. *SEM micrographs of spray-dried composite 65PEG (a) granules and (b) cross-sections.*

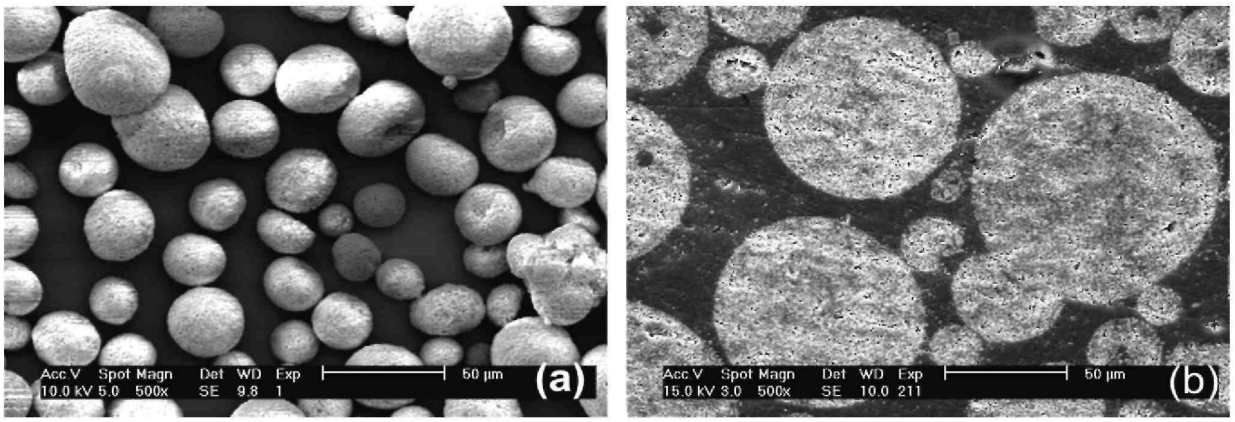

Table 1. *Characteristics of the spray-dried granules: grain size distribution ($d_{0.1}$,$d_{0..5}$, $d_{0..9}$); flowability ($n_{1/2}$, d_{500}/d_0) and apparent density measured by He pycnometry (d_0). See text for details.*

	65PEG			**65PVA**		
	As-sprayed	Sieved	After powder drum	As-sprayed	Sieved	After powder drum
$d_{0.1}$ (µm)	31	38	5	49	33	37
$d_{0.5}$ (µm)	79	79	36	101	71	76
$d_{0.9}$ (µm)	163	146	106	182	141	144
$n_{1/2}$	5	8	-	2	5.5	-
d_{500}/d_0	1.18	1.24	-	1.11	1.09	-
d_0	0.31	0.27	-	0.30	0.29	-

Fig. 5. *Powder-drum experiment: Dynamic angle and standard deviation vs. rotational speed for PEG65 and PVA65 powders.*

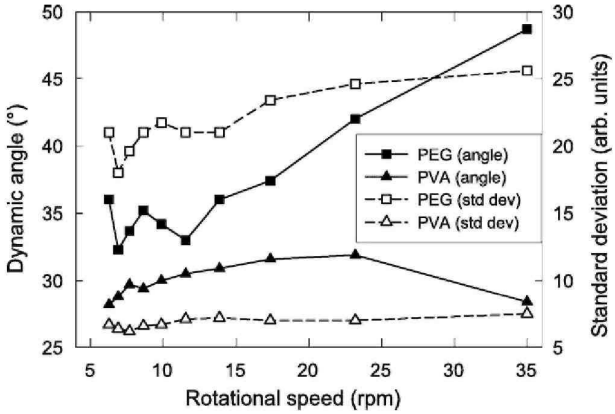

Fig. 6. *Granulometric distribution of the PEG65 powder before (plain line) and after (dashed line) the powder-drum experiment.*

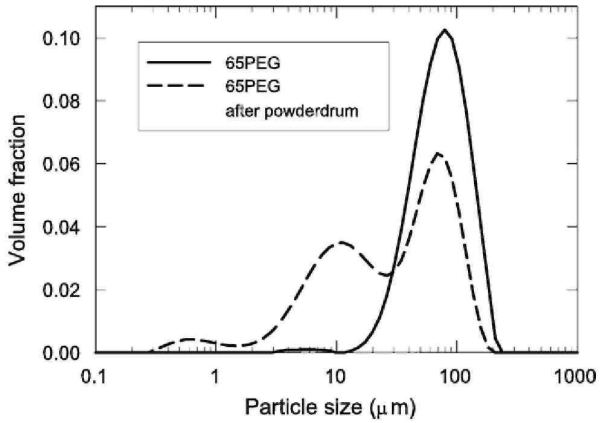

Fig. 7. *SEM micrograph of a cross-section through the coating prepared by reactive plasma spray of the 65PEG powder. Inset: Zoom of an unmelted granule.*

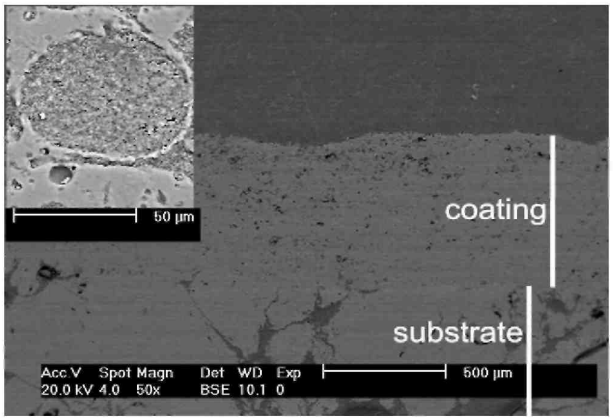

3.3. Reactive plasma spraying

The reactive plasma spraying tests were conducted with a subsonic torch. The maximal power of the torch was selected in order to ensure high thermal plasma-particles transfer for melting of the powder and formation of mullite in the plasma jet before impact on the substrate. Since coating of ceramic substrates (in particular porous refractories) has rarely been studied,[35,36] porous mullite substrates have been used.

Fig. 8. *X-ray diffraction pattern of a coating obtained by reactive plasma spraying of Al_2O_3-SiO_2 granules.*

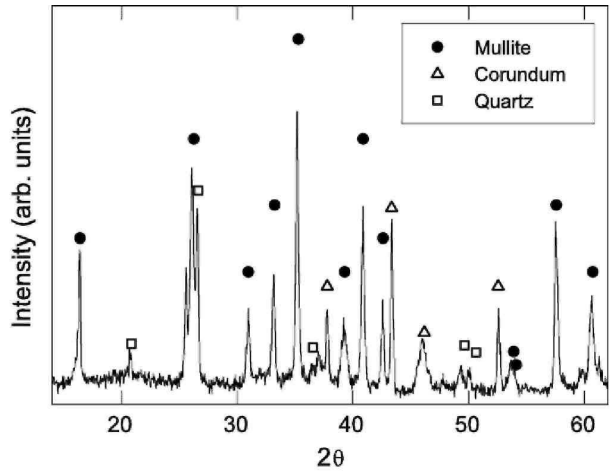

For both spray-dried powders, an adherent coating was formed on the mullite substrate. Fig. 7 shows a scanning electron micrograph of a cross-section through a coating formed by reactive plasma spraying. For the same plasma spraying conditions, the coating obtained with the PVA65 granules is more than four times thicker than the coating obtained with the PEG65 powder. This confirms the practical interest of the characterization conducted above concerning the flowability and cohesion of the spray-dried granules. Fig. 8 shows the X-ray diffractogram of a coating. Crystallographic reflections of mullite, quartz and corundum are identified in the pattern. This shows that mullite formation is possible during the residence time of particles in the plasma jet. However, mullite formation is incomplete. Enhancement of the yield of mullite formation in the plasma jet is likely to require a decrease of the composite granule size below 100 µm and a further optimization of plasma spraying conditions.

4. Conclusion

In this work we have used a combination of ζ-potential and sedimentation measurements in order to determine the pH value and optimum APMA dispersant amount to ensure the stabilisation of high solid loading Al_2O_3+SiO_2 suspensions. Silica suspensions are most stable at basic pH whereas alumina suspensions are stable at acidic pH. The addition of ammonium polymetacrylate makes it possible to stabilise alumina and prepare a stable 50 wt% alumina + silica suspension at pH 10. After addition of 2 wt% binder (PEG or PVA), the viscosity of the suspension remains low and the delay before sedimentation (~4 h) is sufficient for the alumina + silica suspension to be stable during the spray drying process.

Spray-dried composite powders produced from the alumina+silica suspensions are dense spherical particles. The mean particle size depends on the type of binder added to the suspension. The composite granules prepared with PVA have the best fiowability while the granules prepared with PEG binder suffer from a lack of intra-granule cohesion. Reactive plasma spraying of the spray-dried composite shows the possibility to form mullite in the plasma jet before impact of the particles on ceramic substrate. Optimization of the mullite formation yield will need further optimization, such as modification of the spray-drying conditions to obtain smaller granules (<100µm) and optimization of the plasma-spraying parameters.

Acknowledgments

The PowderPaQ and the PowderDrum instruments for physical characterization of the powders are developed by the APTIS group (http://www.aptis.ulg.ac.be). The authors are grateful to FIB Services SA (Baudour, Belgium) and General Metal Alloys Intl (Harzé, Belgium). The authors thank the Laboratoire de Génie Chimique (University of Liège - Prof. J.P. Pirard) for access to the He picnometry measurement system.

References

1. Fauchais, P., Understanding plasma spraying. *J. Phys. D: Appl. Phys*., 2004, **37**, 86-108.

2. Cao, X. Q., Vassen, R. and Stoever, D., Ceramic materials for thermal barrier coatings. *J. Eur. Ceram. Soc*, 2004, **24**, 1-10.

3. Goberman, D., Sohn, Y. H., Shaw, L., Jordan, E. and Gell, M., Microstructure development of Al_2O_3-13 wt.% TiO_2 plasma sprayed coatings derived from nanocrystalline powders. *Acta Mater*., 2002, **50**, 1141-1152.

4. Song, R. G., Hydrogen permeation resistance of plasma-sprayed Al_2O_3 and Al_2O_3-13 wt.%TiO_2 ceramic coatings on austenic stainless stee1. *Surf. Coat. Technol,* 2003, **168,** 191-194.

5. Funke, C., Mailand, J. C., Siebert, B., Vassen, R. and Stöver, D., Characterisation of ZrO_2-7 wt.% Y_2O_3 thermal barrier coatings with different porosities and FEM analysis of stress redistribution during thermal cycling of TBCs. *Surf. Coat. Technol,* 1997, **94-95,** 106-111.

6. Vassen, R., Cao, X., Tietz, F., Basu, D. and Stöver, D., Zirconates as new materials for thermal barrier coatings. *J. Am. Ceram. Soc*, 2000, **83**, 2023-2028.

7. Seifert, S., Litovsky, E., Kleiman, J. L. and Heimann, R. B., Thermal resistance and apparent thermal conductivity of thin plasma-sprayed mullite coatings. *Surf. Coat. Techno*l., 2006, **200,** 3404-3410.

8. Pawlowski, L., *The science and engineering of thermal spray coating.* Wiley, New York, 1995.

9. Lukasiewicz, S. J., Spray-drying ceramic powders. *J. Am. Ceram. Soc*., 1989, **72,** 617-624.

10. Cao, X. Q., Vassen, R., Schwartz, S., Jungen, W., Tietz, F. and Stoëver, D., Spray-drying of ceramics for plasma-spray coating. *J. Eur. Ceram. Soc*., 2000, **20,** 2433-2439.

11. Tsetsekou, A., Agrafiotis, C., Leon, I. and Milias, A., Optimization of the rheological properties of alumina slurries for ceramic processing applications. Part II: spray-drying. *J. Eur. Ceram. Soc,* 2001, **21,** 493-506.

12. Bertrand, G., Filiatre, C., Mahdjoub, H., Foissy, A. and Coddet, C., Influence of slurry characteristics on the morphology of spray-dried alumina powders. *J. Eur. Ceram. Soc.,* 2003, **23**, 263-271.

13. Mahdjoub, H., Roy, P., Filiatre, C., Bertrand, G. and Coddet, C., The effect of the slurry formulation upon the morphology of spray-dried yttria stabilised zirconia particles. *J. Eur. Ceram. Soc.,* 2003, **23**, 1637-1648.

14. Bertrand, G., Roy, P., Filiatre, C. and Coddet, C., Spray-dried ceramic powders: a quantitative correlation between slurry characteristics and shapes of the granules. *Chem. Eng. Sci.,* 2005, **60,** 95-102.

15. Roy, P., Bertrand, G. and Coddet, C., Spray-drying and sintering of zirconia based hollow powders. *Powder Technol*., 2005, **157,** 20-26.

16. Schneider, H., Okada, K. and Pask, J. A., *Mullite and mullite ceramics.* Wiley, New York, 1994.

17. Schmücker, M., Schneider, H., Poorteman, M., Cambier, F. and Meinhold, R., Constitution of mullite glasses produced by ultra-rapid quenching of plasma-sprayed melts. *J. Eur. Ceram. Soc.,* 1995, **15,** 1201-1205.

18. Fisher, J. G., Chang, K., James, P. F, Messe, P. F. and Davies, H. A., Ceramic flakes formation in the aluminosilicate system by plasma spraying. *J. Mater. Sci.,* 2005, **40,** 1625-1632.

19. Hunter, R. J., Recent development in the electroacoustic characterisation of colloidal suspensions and emulsions. *Colloids Surf., A,* 1998,**141,** 37-65.

20. Greenwood, R., Review of the measurement of zeta potentials in concentrated aqueous suspensions using electroacoustics. *Adv. Colloid Interface Sci.,* 2003, **106,** 55-81.

21. Mengual, O., Meunier, G., Cayre, I., Puech, K. and Snabre, P., Characterisation of instability of concentrated dispersion by a new optical analyser: the TURBISCAN MA 1000. *Colloids Surf*., *A,* 1999, **152,** 111-123.

22. Vie, R., Azema, N., Quantin, J. C., Touraud, E. and Fouletier, M., Study of suspension settling: an approach to determine suspension classification and particle interactions. *Colloids Surf*., *A*, 2007, **298,** 192-200.

23. Lumay, G., Vandewalle, N., Bodson, C., Delattre, L. and Gerasimov, O., Linking compaction dynamics to the flow properties of powders. *Appl Phys. Lett*., 2006, **89,** 093505 [3 pages].

24. Boufi, S., Baklouti, S., Pagnoux, C. and Baumard, J.-F., Interaction of cationic and anionic polyelectrolyte with SiO_2 and Al_2O_3 powders. *J. Eur. Ceram. Soc*., 2002, **22,** 1493-1500.

25. Baklouti, S., Pagnoux, C., Chartier, T. and Baumard, J. F., Processing of aqueous *a*-Al_2O_3, α-SiO_2, α-SiC suspensions with polyelectrolytes. *J. Eur. Ceram. Soc*., 1997, **17,** 1387-1392.

26. Kim, D. J. and Kim, H., Dependence of the rheological behaviour of electrostatically stabilized alumina slurries on pH and solid loading. *J. Mater. Sci*., 1998, **33**, 2931-2935.

27. Cesarano, J. and Aksay, I. A., Stability of aqueous α-Al_2O_3 suspensions with poly(mefhacrylic acid) polyelectrolyte. *J. Am. Ceram. Soc*., 1988, **71,** 250-255.

28. Beattie, J. K. and Djerdjev, A., Rapid electroacoustic method for monitoring dispersion: zeta potential titration of alumina with ammonium poly(mefhacrylate). *J. Am. Ceram. Soc*., 2000, **83**, 2360-2364.

29. Singh, P. B., Bhattacharjee, S., Besra, L. and Sengupta, D. K., Electrokinetic and adsorption studies of alumina suspensions using Darvan C as dispersant. *J. Colloid Interface Sci*., 2005, **289,** 592-596.

30. Saranavan, L. and Subramanian, S., Surface chemical studies on the competitive adsorption of poly(ethylene glycol) and ammonium poly (methacrylate) onto alumina. *J. Colloid Interface Sci*., 2005, **284,** 363-377.

31. Romdhane, M. R., Boufi, S., Baklouti, S., Chartier, T. and Baumard, J.-F, Dispersion of $A_{l2}O_3$, suspension with acrylic copolymers bearing car-boxylic groups. *Colloids Surf., A,* 2003, **212,** 271-283.

32. Khan, A. U., Briscoe, B. J. and Luckam, P. F, Interaction of binders with dispersant stabilised alumina suspensions. *Colloids Surf., A,* 2000, **161,** 243-257.

33. Van Krevelen, D. W. and Messing, G. L., *Properties of polymers* (3*rd ed.*). Elsevier, Amsterdam, 1990.

34. Nies, C. W. and Messing, G. L., Plasma-sprayed graded ceramic coatings on refractory materials for improved chemical resistance. *J. Am. Ceram. Soc,* 1984, **67,** 301-304.

35. Bolelli, G., Cannillo, V., Lugli, C., Lusvarghi, C. andManfredini, T., Plasma-sprayed graded ceramic coatings on refractory materials for improved chemical resistance. *J. Eur. Ceram. Soc*., 2006, **26,** 2561-2579.

36. Bartuli, C., Lusvarghi, L., Manfredini, T. and Valente, T., Thermal spraying to coat traditional ceramic substrates: case studies. *J. Eur. Ceram. Soc*., 2007, **27,** 1615-1622.